SUPPLEMENTARY APPENDIX

SUPPLEMENTARY METHODS

Cigarette smoke exposure in ferrets

Age and gender-matched wild-type ferrets [*Mustela putorius furo*, females (0.6–0.8), males (1.2–2.0) kg in body weight] were procured from Marshall BioResources and randomly assigned to whole cigarette smoke exposure or air control groups. Following a brief period of acclimatization and training, ferrets were restrained in customized male and female nose-only exposure tubes and a 24-port plenum connected to the mainstream smoke output. Ferrets were exposed to 60 min of smoke from 3R4F research cigarettes (Univ. of Kentucky, Lexington, KY), twice daily for six months. Cigarette smoke was generated by an automated cigarette smoking apparatus (TSE Systems, Chesterfield, MO) with a 24-cigarette auto-loading carousel. An in-line gas analyzer for oxygen, carbon monoxide, and particulate matter provided real-time estimates of cigarette smoke intensity and ensured accurate and safe exposure of animals. Animals were monitored continuously, and analytics demonstrated particulate matter (200 µg/l of total particulate matter) and CO levels (~1-3%) typical of other animal exposure systems.

Ferret pharmacokinetics

Ferrets were administered GLPG2196 orally as a single esophageal gavage at a dose of 5 or 30 mg/kg provided as a nanosuspension at 100 mg/ml. Ferrets were then anesthetized before whole blood samples were collected via tail vein at 1, 3, 6, and 24 hrs post-administration. Samples were centrifuged, and the resulting plasma samples kept frozen at -80°C until LC-MS/MS analysis (AB Sciex® API6500 QTrap).

Oral administration of CFTR modulators in a ferret model of COPD

Following six months of cigarette smoke exposure, ferrets were administered GLPG2196 (30 mg/kg) orally once daily for one month followed by post-treatment assessments. As a control, vehicle was administered at the same frequency. Smoke exposure was continued throughout the treatment period.

Ferret short-circuit current (Isc)

Assessments of Isc in primary ferret bronchial epithelial (FBE) cells and *ex vivo* ferret trachea were carried out using MC8 clamps and P2300 Ussing chambers (Physiologic Instruments, San Diego, CA) under voltage-clamp conditions (1). For experiments using FBE cells, cells were cultured at air-liquid interface and treated with GLPG2196 up to a dose of 10 μM before the addition of NaCl Ringer's solution (115 mM NaCl, 25 mM $NaHCO_3$, 2.4 mM KH_2PO_4, 1.24 mM K_2HPO_4, 1.2 mM $CaCl_2$, 1.2 mM $MgCl_2$, and 10 mM D-glucose (pH 7.4)) to both apical and basolateral sides of the monolayer. Bath solutions were then oxygenated (95%O_2:5% CO_2) and chambers were maintained at 37°C. To augment the sensitivity of Isc measurements, when indicated the mucosal bathing solutions were replaced with low Cl^- Ringer's comprised of 1.2 NaCl and 115 Na^+ gluconates, in addition to the other components of Ringer's solution detailed above. Amiloride (100 μM, to block ENaC), forskolin (to induce cAMP-mediated stimulation of CFTR) and $CFTR_{Inh}$-172 (10 μM) or GlyH101 (20 μM), each to inhibit CFTR-dependent Isc, were subsequently added as indicated; in other studies, GLPG2196 was added at the concentration shown.

For analysis of tracheal Isc, trachea were harvested from euthanized wild-type ferrets and treated with cigarette smoke extract (1% in DMSO) or vehicle (DMSO) control. Some studies included GLPG2196 (10 μM) or vehicle. The mucosal layer was then dissected, and tissues were mounted on P2307 tissue mounts. Isc was assessed as described for FBE

monolayers, except for the initial addition of amiloride (100 μM; to inhibit residual Na^+ current) before the addition of the low Cl^- solution.

Ferret nasal potential difference (NPD)

Ferrets were anesthetized, after which a small amount of lidocaine gel was placed on the exterior of the nare to inhibit sneeze response. The left nare was cannulated with PE-90 tubing pulled to a tip diameter of 0.30 mm. The potential difference anode was connected via an agar-filled 18G needle to a calomel/KCl cell connected to a high impedance voltmeter (VF-1; World Precision Instruments). Ringer's solution (baseline measurement), Ringer's plus amiloride (100 μm), a Cl^- free solution containing K_2HPO_4 (2.4 mM), KH_2PO_4 (0.4 mM), Na gluconate (115 mM), $NaHCO_3$ (25 mM), and Ca_2 gluconate (1.24 mM) with amiloride, and a Cl^--free solution plus forskolin (20 μM) were sequentially perfused at a rate of 3.0 ml/hr for at least 6 min each or until a stable potential was achieved. A Powerlab analog to digital converter and LabChart 7.0 software (AD Instruments) was used for analysis, as previously described for human studies (2). CFTR-dependent chloride transport was measured as the change in potential difference following perfusion with chloride-free solution plus forskolin.

μOCT imaging

Video-rate μOCT images (acquired at a frame rate of 40 frames/second) of tracheal explants from ferrets were captured promptly after excision for analysis of airway functional microanatomy using ImageJ (NIH, Bethesda, MD) and MATLAB software (MathWorks, Natick, MA) (3-5). For imaging, tissues were placed on gauze saturated in warmed DMEM (Gibco, Waltham, MA) containing the prostaglandin signaling inhibitor indomethacin (1 μM; Sigma-Aldrich, St. Louis, MO) and allowed to stabilize for 15-30 min at physiologic temperature and 5% CO_2 before imaging.

Particle tracking microrheology analysis

To determine mucus viscosity using particle tracking microrheology **(**PTM) (3, 6), ferret tracheal explants that were imaged by μOCT were subsequently plugged at each end to foster the accumulation of mucus, which was further stimulated by a 2-hr treatment with carbachol (10 μM) and phenylephrine (20 μM; Sigma-Aldrich). Mucus was then collected by pipette, and polyethylene glycol–polystyrene (PEG-PS; 500-nm or 1-μm) particles were applied at a 1:10 v/v dilution. Samples (10 μL) were placed on coverslips, which were allowed to sit for 60 min at room temperature before imaging by μOCT or fluorescent microscopy (Nikon TE200, Nikon Instruments, Melville, NY. ImageJ (NIH) and the SpotTracker plug-in were used to analyze images to acquire particle tracks for analysis of MSD, corrected for spurious bulk motion using custom MATLAB procedures, and dynamic viscosity, derived by applying the generalized Stokes-Einstein relation to MSD (6).

μCT imaging

We conducted non-contrast CT imaging of ferrets under inhaled isoflurane anesthesia and retrospectively gated for a single inspiratory phase of respiration using a μCT scanner (MiLabs, Utrecht, Netherlands) and semi-automated measurements as previously described (7). Airway wall metrics of the right and left upper lobe were calculated using a semi-automated algorithm by an investigator blinded to treatment assignment (7).

Necropsy and histopathologic analysis

Anesthetized ferrets were euthanized by exsanguination when in clinical distress or at the end of the study. Separate lung lobes were designated for histopathology and biochemical analysis of CFTR expression and inflammation. The left lung was inflated by instilling 70%

alcoholic formalin to a pressure of 25 cm of water and fixed in excess formalin for a minimum of 48 hrs before being sectioned and embedded in paraffin. Tissue sections were examined by an expert veterinary pathologist in direct comparison to controls. Quantitative morphometry was performed by an expert veterinary pathologist blinded to treatment assignment as described previously (8).

CFTR protein expression by immunoblot analysis

Frozen lung segments were washed with PBS and lysed with Triton X-100 buffer [1% Triton X-100, 150 mM NaCl, 5 mM EDTA, and 50 mM Tris/HCl (pH 7.4)] containing 1X protease inhibitor cocktail (Halt Protease Inhibitor Cocktail Kit, Thermo Scientific Pierce Protein Biology Products) and EDTA for 45 min on ice. Following centrifugation (20000 *g* for 10 min at 4°C), pellets were discarded and protein concentration measured using BCA protein assay (Thermo Scientific Pierce). Equal amounts of protein (15–30 µg) were incubated in 4× Laemmli buffer with 10% 2-mercaptoethanol at 37°C for 15 min, electrophoresed through a 4–12% SDS/PAGE gel, and transferred to PVDF membrane. Blocking was in 1× PBS, 0.1% Tween-20, and 5% (w/v) non-fat dried skimmed milk powder for 30 min at room temperature (23°C) followed by overnight incubation at 4°C with the 529 anti-CFTR antibody in blocking buffer. After three washes (1× PBS plus 0.1% Tween-20), membranes were incubated with secondary antibody conjugated to horseradish peroxidase followed by chemiluminescence with SuperSignal West Femto or West Pico Chemiluminescent Substrate (Thermo Scientific Pierce). Membranes were imaged using ChemiDoc XRS HQ (Bio-Rad Laboratories) or Kodak Biomax MR film. Densitometry was performed with Quantity One or ImageLab software (Bio-Rad Laboratories).

RNA isolation, cDNA synthesis, and real-time quantitative RT-PCR

RNA was extracted from representative lung specimens from ferrets exposed to air or cigarette smoke for six months using RNAeasy Kit (Qiagen) according to the manufacturer's

recommendations. Isolated RNA was reverse-transcribed into cDNA using Iscript cDNA synthesis kit (Bio-Rad Laboratories). Real-time PCR was performed and quantified with a SYBR Green containing PCR mix (Bio-Rad Laboratories). Ferret CFTR was amplified using forward primer GGAAAATTAAGCACAGTGGAAGAA (Life Technologies) and reverse primer GGTGCCAGGCATGATCC. Human rRNA primers (A&B Applied Biosystems) were amplified as reference controls. A calibrator sample from human Calu-3 epithelial cells was included in every run to correct for inter-run variability. *Cq* values were determined by using the A&B Applied Biosystems software, and average CFTR expression for each group was considered for statistical analysis.

Reagents

GLPG2196 was provided by Galapagos. Forskolin (Calbiochem) and GlyH101 (Santa Cruz Biotechnology) were obtained as noted. All other chemicals were obtained from Sigma-Aldrich.

Statistics

Descriptive statistics were reported as mean ± SEM unless indicated otherwise (i.e. µCT imaging where the number of airways is large) and compared using Student's t-test or ANOVA, as appropriate. Non-parametric statistics were used when N's were small or data were not normally distributed. Post-hoc tests for multiple comparisons following ANOVA were calculated only if ANOVA was significant and corrected for multiple comparisons. All statistical tests were two-sided and were performed at a 5% significance level (i.e., $\alpha = 0.05$) using GraphPad Prism software (Version 7 or greater). Data are presented as mean ± SEM unless indicated otherwise.

Study approval

All animal protocols used in this work were reviewed and approved by the UAB Institutional Animal Care and Use Committee.

SUPPLEMENTARY FIGURES

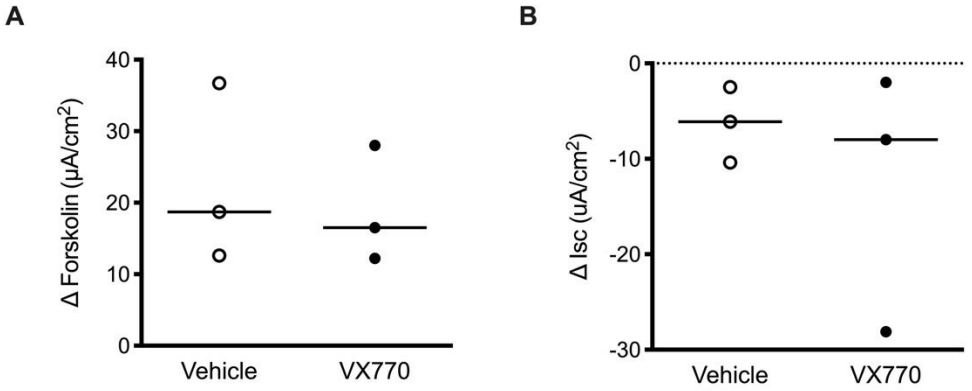

Supplemental Figure S1. Ivacaftor does not activate wild-type CFTR in ferrets *ex vivo*. Ferret tracheal segments were mounted in Ussing chambers for electrophysiologic analysis. The experiment included serial addition of amiloride (100 μM), chloride secretory gradient with amiloride, followed by forskolin (100 nM), then DMSO vehicle or ivacaftor (VX770, 10 μM). **(A)** Mean change in CFTR-dependent short-circuit current (Isc) after addition of positive control, forskolin (neither vehicle nor VX770 added). **(B)** Mean change in Isc after subsequent addition of vehicle or ivacaftor. Negative currents indicate no subsequent stimulation. *n* = 3 tracheal segments derived from different ferrets, Mann-Whitney U test.

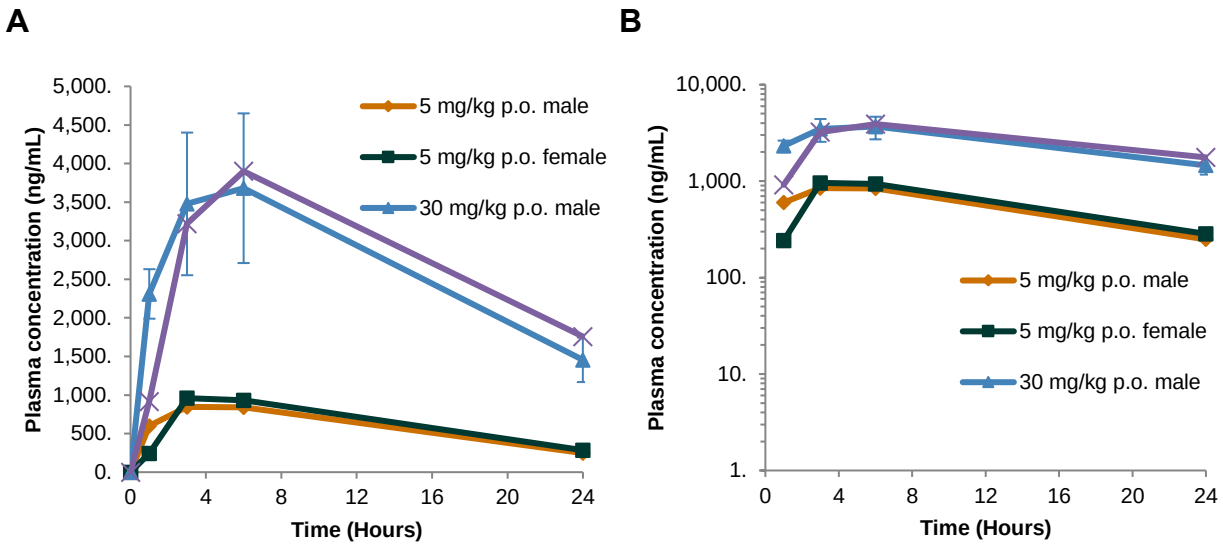

Supplemental Figure S2. Plasma concentration of GLPG2196 over time in ferrets. **(A)** Linear plot and **(B)** semi-logarithmic plot showing mean (±SEM) plasma concentration of GLPG2196 in male and female ferrets over 24 hours. GLPG2196 was administered orally as a single esophageal gavage at both 5 and 30 mg/kg. *n* = 2-3/group.

SUPPLEMENTARY REFERENCES

1. Kaza N, Raju SV, Cadillac JM, Trombley JA, Rasmussen L, Tang L, Dohm E, Harrod KS, Rowe SM. Use of ferrets for electrophysiologic monitoring of ion transport. *PLoS One* 2017; 12: e0186984.
2. Solomon GM, Konstan MW, Wilschanski M, Billings J, Sermet-Gaudelus I, Accurso F, Vermeulen F, Levin E, Hathorne H, Reeves G, Sabbatini G, Hill A, Mayer-Hamblett N, Ashlock M, Clancy JP, Rowe SM. An international randomized multicenter comparison of nasal potential difference techniques. *Chest* 2010; 138: 919-928.
3. Lin VY, Kaza N, Birket SE, Kim H, Edwards LJ, LaFontaine J, Liu L, Mazur M, Byzek SA, Hanes J, Tearney GJ, Raju SV, Rowe SM. Excess mucus viscosity and airway dehydration impact COPD airway clearance. *Eur Respir J* 2020; 55.
4. Liu L, Shastry S, Byan-Parker S, Houser G, Chu K, Birket SE, Fernandez CM, Gardecki JA, Grizzle W, Wilsterman EJ, Sorscher EJ, Rowe SM, Tearney GJ. An Autoregulatory Mechanism Governing Mucociliary Transport is Sensitive to Mucus Load. *Am J Respir Cell Mol Biol* 2014.
5. Liu L, Chu KK, Houser GH, Diephuis BJ, Li Y, Wilsterman EJ, Shastry S, Dierksen G, Birket SE, Mazur M, Byan-Parker S, Grizzle WE, Sorscher EJ, Rowe SM, Tearney GJ. Method for quantitative study of airway functional microanatomy using micro-optical coherence tomography. *PLoS One* 2013; 8: e54473.
6. Chu KK, Mojahed D, Fernandez CM, Li Y, Liu L, Wilsterman EJ, Diephuis B, Birket SE, Bowers H, Martin Solomon G, Schuster BS, Hanes J, Rowe SM, Tearney GJ. Particle-Tracking Microrheology Using Micro-Optical Coherence Tomography. *Biophys J* 2016; 111: 1053-1063.
7. Stanford D, Kim H, Bodduluri S, LaFontaine J, Byzek SA, Schoeb TR, Harris ES, Nath HP, Bhatt SP, Raju SV, Rowe SM. Airway Remodeling in Ferrets with Cigarette Smoke Induced COPD using microCT Imaging. *Am J Physiol Lung Cell Mol Physiol* 2020.

8. Raju SV, Kim H, Byzek SA, Tang LP, Trombley JE, Jackson P, Rasmussen L, Wells JM, Libby EF, Dohm E, Winter L, Samuel SL, Zinn KR, Blalock JE, Schoeb TR, Dransfield MT, Rowe SM. A ferret model of COPD-related chronic bronchitis. *JCI Insight* 2016; 1: e87536.